APL Photonics

Cumulative plasma effects in cavity-enhanced high-order harmonic generation in gases

Cite as: APL Photonics 3, 101301 (2018); https://doi.org/10.1063/1.5037196
Submitted: 22 April 2018 . Accepted: 02 July 2018 . Published Online: 02 August 2018

Tobias Saule, Maximilian Högner, Nikolai Lilienfein, Oliver de Vries, Marco Plötner, Vladislav S. Yakovlev, Nicholas Karpowicz, Jens Limpert, and Ioachim Pupeza

Cumulative plasma effects in cavity-enhanced high-order harmonic generation in gases

Tobias Saule,[1,2] Maximilian Högner,[1,2] Nikolai Lilienfein,[1,2] Oliver de Vries,[3] Marco Plötner,[3] Vladislav S. Yakovlev,[1,2] Nicholas Karpowicz,[1] Jens Limpert,[4,5,6] and Ioachim Pupeza[1,a]

[1]*Max-Planck-Institute of Quantum Optics, Hans-Kopfermann-Str. 1, 85748 Garching, Germany*
[2]*Ludwig-Maximilians-University Munich, Am Coulombwall 1, 85748 Garching, Germany*
[3]*Fraunhofer Institute for Applied Optics and Precision Engineering, Albert-Einstein-Str. 7, 07745 Jena, Germany*
[4]*Friedrich-Schiller-University Jena, Institute for Applied Physics, Albert-Einstein-Str. 15, 07745 Jena, Germany*
[5]*Helmholtz-Institute Jena, Fröbelstieg 3, 07743 Jena, Germany*
[6]*Active Fiber Systems GmbH, Wildenbruchstr. 15, 07745 Jena, Germany*

(Received 22 April 2018; accepted 2 July 2018; published online 2 August 2018)

Modern ultrafast laser architectures enable high-order harmonic generation (HHG) in gases at (multi-) MHz repetition rates, where each atom interacts with multiple pulses before leaving the HHG volume. This raises the question of cumulative plasma effects on the nonlinear conversion. Utilizing a femtosecond enhancement cavity with HHG in argon and on-axis geometric extreme-ultraviolet (XUV) output coupling, we experimentally compare the single-pulse case with a double-pulse HHG regime in which each gas atom is hit by two pulses while traversing the interaction volume. By varying the pulse repetition rate (18.4 and 36.8 MHz) in an 18.4-MHz roundtrip-frequency cavity with a finesse of 187, and leaving all other pulse parameters identical (35-fs, 0.6-μJ input pulses), we observe a dramatic decrease in the overall conversion efficiency (output-coupled power divided by the input power) in the double-pulse regime. The plateau harmonics (25–50 eV) exhibit very similar flux despite the twofold difference in repetition rate and average power. We attribute this to a spatially inhomogeneous plasma distribution that reduces the HHG volume, decreasing the generated XUV flux and/or affecting the spatial XUV beam profile, which reduces the efficiency of output coupling through the pierced mirror. These findings demonstrate the importance of cumulative plasma effects for power scaling of high-repetition-rate HHG in general and for applications in XUV frequency comb spectroscopy and in attosecond metrology in particular. https://doi.org/10.1063/1.5037196

INTRODUCTION

Frequency upconversion of ultrashort, intense visible/near-infrared (VIS/NIR) laser pulses to the extreme-ultraviolet (XUV) spectral region via high-order harmonic generation (HHG) in noble gases lies at the core of table-top sources of broadband, coherent XUV radiation.[1] Customarily, the master-oscillator-power-amplifier (MOPA) systems driving HHG operate at pulse repetition rates in the range of several kHz, as a result of the trade-off between the high peak powers necessary for HHG and constraints on the average power in amplifiers. At these pulse repetition rates, the atoms interacting with the HHG-driving pulses usually leave the interaction volume long before the arrival of the subsequent pulse. In this highly relevant and widespread single-pass regime, the process of HHG has

[a]ioachim.pupeza@mpq.mpg.de

been extensively studied.[1] The recent advent of ultrafast laser technologies affording pulses suitable for HHG at repetition rates in the multi-MHz range[2–16] has opened the door to applications barely fathomable with the well-established kHz technologies. Among those, precision spectroscopy with XUV frequency combs[5,6,17] and high-speed multi-dimensional laser-dressed XUV photoemission spectroscopy[18,19] are particularly prominent examples. However, for these repetition rates, the period between two pulses becomes comparable to—or shorter than—the time atoms take to travel through the volume where they can interact with the laser pulses. Consequently, the quantitative study of the cumulative plasma effects arising from the interaction of each atom with multiple pulses is necessary for designing and optimizing applications in this high-repetition-rate regime of HHG.

In this paper, we present an experimental comparison of HHG in the single-pulse (SP) regime (each atom is hit only once) with the case in which each atom interacts with two pulses of the driving laser (double-pulse, DP). To this end, we set up an 18.4-MHz-repetition-rate femtosecond enhancement cavity with either one circulating pulse or two circulating pulses and systematically evaluated the spectra and flux of the XUV radiation coupled out through a pierced mirror following the HHG focus. To investigate the cumulative plasma effects on the HHG process, the only parameter varied between these two cases was the pulse repetition frequency (18.4 MHz or 36.8 MHz), while the pulse parameters in the cavity (pulse energy, duration, and spatial profile) were kept constant within the accuracy of the diagnostics. To ensure that optimum generation conditions for each harmonic order and repetition rate are covered by the experiment, we performed complete scans of the target gas density and nozzle position along the optical axis. We observed a dramatic dependence of the conversion efficiency on the repetition rate, which can be attributed to cumulative plasma effects in the HHG target.

EXPERIMENTAL SETUP

In femtosecond enhancement cavities (EC), the pulses of a mode locked laser are coherently stacked and their energy is enhanced by up to several orders of magnitude. Peak intensities of several 10^{13} W/cm^2 at a cavity focus can be achieved, permitting HHG at repetition rates of several tens of MHz.[5–12,18–22] ECs have been successfully used for a number of seminal HHG experiments at high repetition frequencies like direct XUV frequency comb spectroscopy,[6] the determination of the coherence time of XUV frequency combs[5] at 154 MHz repetition rate, and the generation of 100-eV frequency combs.[10,11] However, despite affording circulating pulses shorter than 10 optical cycles with average powers on the 10-kW level,[10–12] the number of XUV photons per pulse obtained with cavity-enhanced HHG cannot compete with direct, single-pass HHG.[3] These results indicate that the presence of gas ionized by the preceding driving pulses reduces the HHG efficiency (per pulse), and the scaling of XUV power with the laser repetition rate deviates strongly from a linear dependence in this regime. For a direct and quantitative investigation of this effect, we designed an EC such that its repetition period equals the traversing time of the gas atoms through the interaction volume. Thus, when seeded with twice its fundamental repetition rate, each atom interacts with two pulses.

The experimental setup is shown in Fig. 1(a). The frontend seeding the enhancement cavity is described in Ref. 25. In brief, a titanium-sapphire (Ti:Sa) seed oscillator emits a 73.6-MHz pulse train, whose repetition frequency can be picked by an integer factor.[23] Chirped-pulse amplification employing Yb-doped fibers delivers 250-fs pulses with an energy of more than 1 μJ for repetition rates down to a few MHz. Spectral broadening in a large-mode-area (LMA) fiber with a 25-μm core and subsequent temporal compression with chirped mirrors (CM) deliver 0.6-μJ, 35-fs pulses spectrally centered at 1030 nm, with repetition-rate-independent characteristics.[25] These pulses impinge on a 16.3-m (corresponding to the single round-trip distance for a repetition rate of 18.4-MHz) EC with an input coupler transmission of 3%. The EC has a finesse of 187 (considering the losses of 0.32% at the 150-μm pierced output-coupling mirror). Compared to other output-coupling methods, this geometric method allows for broadband XUV output coupling of photon energies of 100 eV and higher and provides phase-locked collinear NIR pulses.[18]

In the experiments reported here, the EC was seeded with pulse trains of either 18.4 MHz or 36.8 MHz, resulting in comparable intra-cavity pulse parameters [Figs. 1(b)–1(d)]. An argon gas

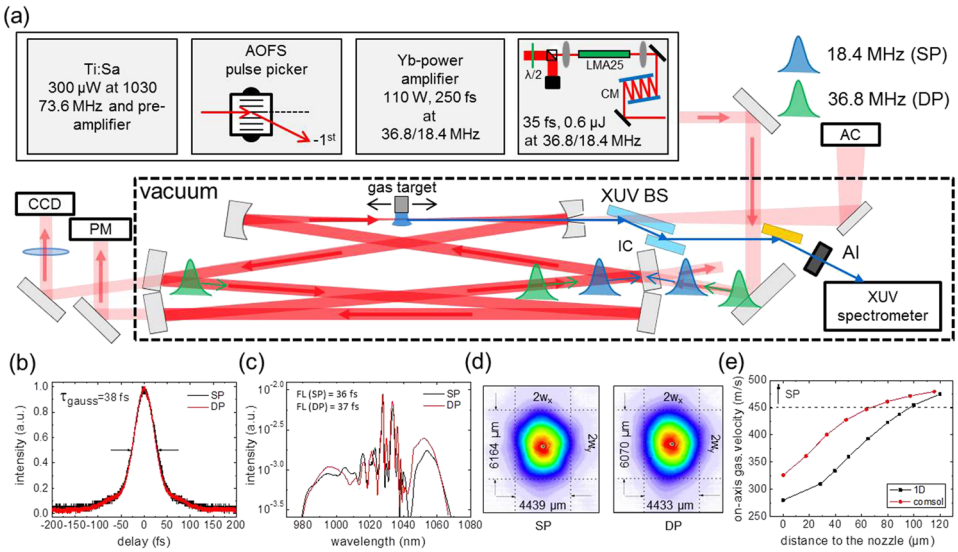

FIG. 1. (a) Experimental setup consisting of a Ti:Sa seed, an acousto-optic frequency shifter (AOFS) pulse picker,[23] an Yb-power-amplifier,[24] spectral broadening, chirped-mirror (CM) compression, and a 16.3-m enhancement cavity with either one (18.4 MHz, SP) circulating pulse or two (36.8 MHz, DP) circulating pulses. The spectral broadening is achieved in a solid-core large-mode-area (LMA) fiber with a 25-μm core diameter providing identical pulses at 36.8 MHz and 18.4 MHz, with 0.6 μJ and 35 fs.[25] The XUV radiation is coupled out through a pierced mirror[11] and guided to an XUV spectrometer by two multi-layer beam splitters (BS). Intracavity pulse parameters in the presence of the nonlinear gas target, for the two repetition rates: (b) autocorrelation (AC, τ_{gauss} = 38 fs), (c) spectrum with Fourier-limits (FL) of 36 fs and 37 fs, respectively, (d) beam profile on the pierced mirror, imaged to the CCD camera. (e) Gas velocity along the flow direction of a 100-μm nozzle, derived by a 1D model[26] and confirmed via Comsol MultiPhysics. Complete replenishment of the gas target within 54 ns (repetition period of the SP regime) is achieved for velocities >450 m/s, at a beam waist of 12.3 μm.

target delivered by a 100-μm fused-silica end-fire nozzle was positioned at the focal region. The gas flow velocity at a distance of ~100 μm from the nozzle orifice was estimated to be 450 m/s [Fig. 1(e)] by a 1D model[26] as well as flow simulations using Comsol MultiPhysics. The curved mirrors of the EC (f = 100 mm) and the position in the stability range were chosen such that the beam waist was 12.3 μm. This results in peak intensities of several 10^{13} W/cm^2 and ensured SP configuration for the 18.4-MHz pulse train, meaning that an atom traverses the $1/e^2$–intensity beam diameter within one repetition period. At 36.8 MHz, the atoms traverse this distance within 2 shots and, thus, we refer to this regime as the double-pulse (DP) configuration. The generated harmonics were coupled out of the cavity through a 150-μm opening in the mirror following the focus[11] and split from the fundamental beam by two multi-layer Nb_2O_5 beam splitters. To prevent hydrocarbon contaminations of the optics, we flushed the two cavity mirrors and two beam splitters subsequent to the XUV generation with ozone. The XUV beam was then directed to a grating spectrometer whose linearity with respect to the XUV flux was confirmed in a previous experiment. To exclude thermal effects in the system, all experiments reported here were performed at a maximum repetition rate of 36.8 MHz, corresponding to average powers of 11 W and 0.6 kW impinging on and circulating in the EC, respectively. For both repetition rates, stable operation of the system under constant conditions was possible for measurement times longer than 10 h.

RESULTS

To study the cumulative effects in a controlled way and to ensure comparable pulse parameters for the two repetition rates, for each data point, we recorded the intracavity average power, the pulse duration, and the beam profile on one mirror, in an actively locked[10] steady state. This measurement also allows for the precise determination of the position of the nozzle with respect to the focus by evaluating the plasma-induced power clamping[20] for different target positions along the cavity beam. This delivers 2D maps for all the intra-cavity parameters regarding the backing pressure and

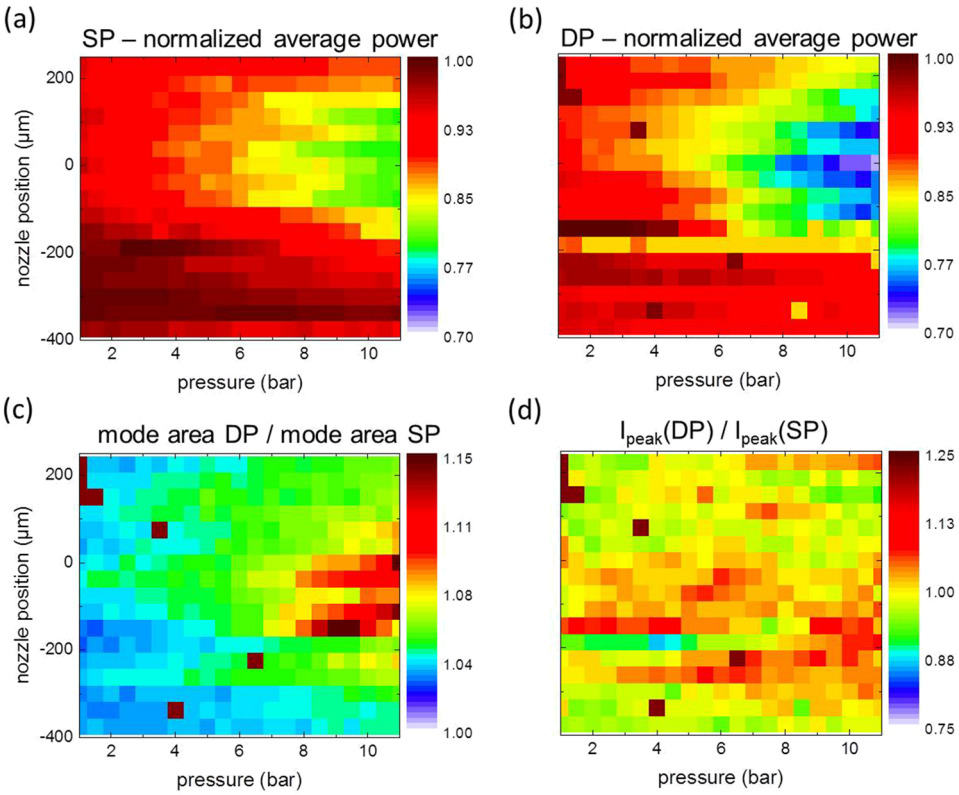

FIG. 2. [(a) and (b)] Normalized intra-cavity average power clamping maps for the SP and the DP, respectively. They demonstrate how the intra-cavity power level clamps as a function of the nozzle position and backing pressure. The experimentally determined focus position (see the text) is set to 0 μm. One immediate observation is that the DP configuration experiences stronger clamping in the focus region. (c) Ratio of the mode area of the DP versus the SP on the pierced mirror. The larger ratios in the focus region stem from changes in the DP mode area, while the relative changes in the SP mode area stay below 2.7%. (d) Ratio of the peak intensities (calculating from the mode size, average power, pulse duration, and target position) for the two repetition rates.

target position; they are depicted in Figs. 2(a)–2(d). Figures 2(a) and 2(b) show the average power in the cavity with the gas target being present, normalized to the average power in the empty cavity for the same input pulse parameters for the SP and the DP, respectively. They demonstrate that cumulative effects affect the cavity operation as the DP configuration clamps to 70% of the linear cavity, whereas the SP only clamps to 80% in the focus. Figure 2(c) illustrates the evolution of the DP cavity eigenmode on the pierced mirror with respect to the SP configuration by showing the ratio of the mode area of the DP to SP case for different experimental parameters. Here, the change in the mode area in the DP dominates the ratio, whereas the changes in the SP contribute little (<2.7%). The map reveals an opposing behavior compared to the average power [see (a) and (b)]. Taking these mode distortions into account, we can calculate the intra-cavity peak intensity by utilizing the mode size, average power, pulse duration, and target position. The data reveal similar values for both repetition rates [see Fig. 2(d)], which fits to the identical XUV cutoff in the following experiments.

With the focus as a reference point for the optical axis and well-characterized experimental conditions, we examined the output coupled XUV flux. Figure 3(a) shows the relative XUV flux per harmonic (integrated counts within one harmonic) for the SP (1st row) and the DP (2nd row) configuration, as a function of the nozzle position and backing pressure, for six different harmonics. The color scales are the same for each harmonic to facilitate the comparison between the two repetition rates. Figure 3(b) shows the XUV spectrum at the gas target pressure and position marked in (a), circles, for both repetition rates, where the flux of the 33rd harmonic is optimal for the SP configuration. In Fig. 3(c), each harmonic is plotted at its optimum values within the maps in

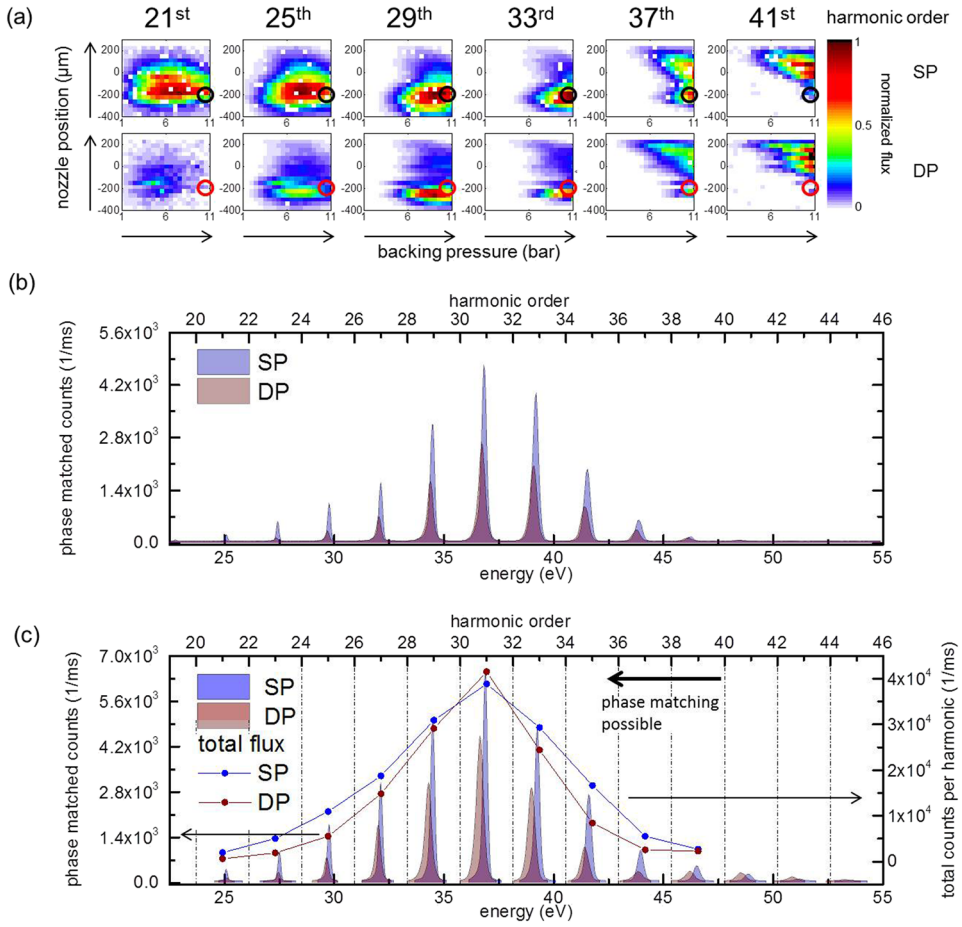

FIG. 3. (a) XUV flux measured as a function of the gas target position and backing pressure, for six different harmonics, for SP (1st row) and DP (2nd row). For each harmonic, the color scales are common to the SP and DP maps; they are normalized to the highest flux. The nozzle position of 0 μm marks the cavity focus determined as explained in the text. (b) XUV spectra for both repetition rates measured for the parameters indicated in (a) by the circles. (c) Stitched XUV spectrum for individually optimized conditions for SP and DP, taken from the positions on the maps with the highest flux. The dots represent the integrated flux within these harmonics.

Fig. 3(a). The data points connected with solid lines depict the counts spectrally integrated over each harmonic order.

DISCUSSION

Figure 3(a) shows that further increasing the pressure does not improve the flux for harmonic orders up to 39, which indicates that we achieved optimized phase matching conditions (under the boundary conditions of the EC) for these harmonics at both repetition rates. The target position was scanned over a large enough range to include the optimum positions.

Evidently, the SP configuration is preferable in terms of the total output coupled flux [Fig. 3(c)] and conversion efficiency. Figure 4(a) depicts the ratio of the XUV flux of the DP configuration and the SP one for each harmonic order. While a ratio of two would correspond to a linear scaling of the XUV flux with the repetition rate (keeping the pulse parameters constant), most harmonics manifest a ratio below unity, i.e., the DP yields even less flux than the SP configuration, despite twice the driving average power. This corresponds to a dramatic decrease in the overall conversion efficiency (output-coupled power divided by seed power) by up to a factor of 4 due to cumulative plasma effects.

At the same time, for all harmonics, the optimum generation conditions (target gas density and position) are very similar for the two repetition rates. This indicates that the ionization fraction in the

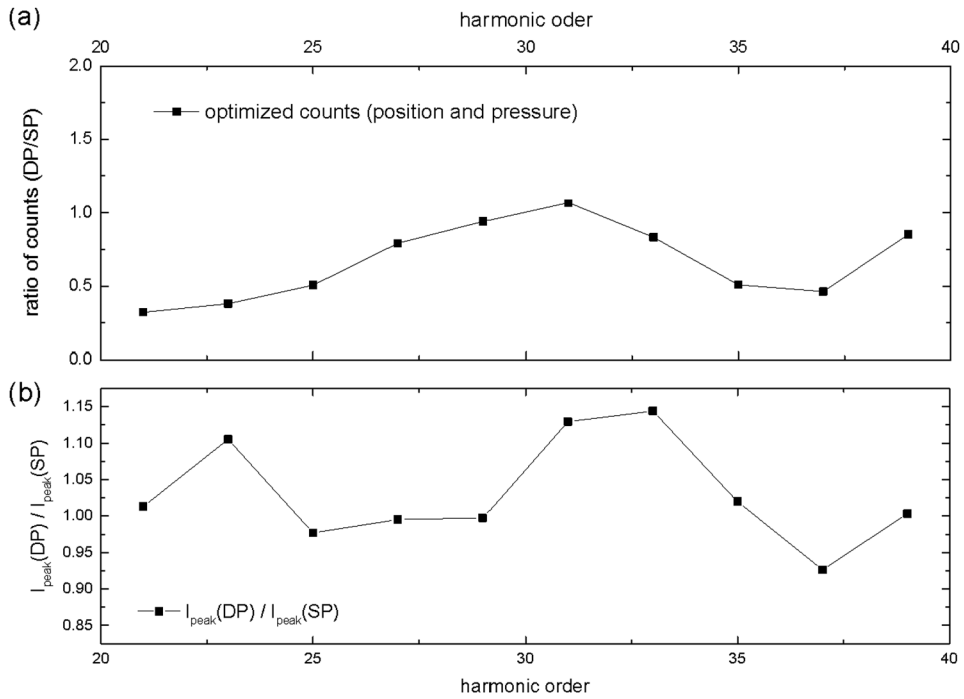

FIG. 4. (a) Ratio of the output coupled flux for the DP versus the SP configuration. A value of 2 corresponds to the same conversion efficiency (output-coupled power divided by the input power) as double the average seed power is available for the DP configuration. (b) Ratio of the calculated peak intensity for the DP versus the SP case. The peak intensity was calculated from the mode size, focusing geometry, intra-cavity pulse duration, and calibrated intra-cavity power.

contributing part of the target gas is similar for both the SP and the DP, and the substantial decrease in flux can rather be attributed to a decrease in the generation volume: in the DP regime, the gas target is spatially partitioned into a part that was already hit by the previous pulse and propagated off-axis, contributing little to the flux (e.g., due to preionization), and a part with "fresh" ground-state gas atoms. This would affect the output coupled flux in two ways: first, fewer atoms contribute to HHG and second, the reduced generation volume results in a larger divergence of the harmonic beam and, thus, a lower output coupling efficiency. To confirm and disentangle these effects, a similar experiment with a Brewster plate[8,12] or a diffraction-based output coupling method[6,7] can be performed. This way the decrease in output coupling efficiency due to changes in the XUV beam profile can be scrutinized and possibly more profound conclusions about the physical processes can be extracted. Another meaningful single-pass experiment could be the generation of high harmonics with two slightly delayed pulses, analyzing the HHG yield and XUV mode profile with respect to the delay.

To exclude that the decrease in the flux in the DP configuration is due to a stronger intensity clamping of the driving field [Fig. 2(a)], we computed the peak intensity in the target for each point of the parameter scan, accounting for the measured pulse duration, cavity mode size, and target position. Figure 2(d) shows the peak intensity ratio between the DP and SP cases. It can be seen that the peak intensity is very similar in the two configurations, even though the average power clamping suggests otherwise. This can be attributed to small changes in the cavity mode size [see Fig. 2(c)]. At optimum parameters for each harmonic, the DP configuration even exhibits a slightly higher peak intensity [see Fig. 4(b)].

In conclusion, these findings elucidate the importance of cumulative plasma effects in multi-pass HHG, whose effects are already significant at the onset of the cumulative regime (two passes). The phase-matched plateau harmonics clamp to the same flux independently of the repetition rate. Our data show that this reduction of XUV flux is not a result of distortions of the circulating IR field. By contrast, we attribute these findings to a spatially inhomogeneous plasma distribution that hinders the output coupling efficiency of the pierced mirror and/or of the HHG generation itself.

For applications requiring multi-MHz, high-photon-energy, high-flux XUV pulses, these findings elucidate the benefit of a single-pulse regime achievable by adapting the repetition rate of the system and/or by speeding up the gas.[7,10] With the same experimental setup, the repetition rate scalability of HHG in solids[27–29] can in principle be examined by replacing the gas target with a thin Brewster plate.

ACKNOWLEDGMENTS

This work was supported by the project MEGAS in the frame of the Fraunhofer-Max-Planck Cooperation and by the German Research Foundation (DFG) via the Munich Centre for Advanced Photonics (MAP).

[1] M. Wegener, *Extreme Nonlinear Optics* (Springer, 2005).
[2] S. Hädrich, J. Rothhardt, M. Krebs, S. Demmler, A. Klenke, A. Tünnermann, and J. Limpert, "Single-pass high harmonic generation at high repetition rate and photon flux," J. Phys. B: At., Mol. Opt. Phys. **49**, 172002 (2016).
[3] S. Hädrich, A. Klenke, J. Rothhardt, M. Krebs, A. Hoffmann, O. Pronin, V. Pervak, J. Limpert, and A. Tünnermann, "High photon flux table-top coherent extreme-ultraviolet source," Nat. Photonics **8**, 779–783 (2014).
[4] S. Hädrich, M. Krebs, A. Hoffmann, A. Klenke, J. Rothhardt, J. Limpert, and A. Tünnermann, "Exploring new avenues in high repetition rate table-top coherent extreme ultraviolet sources," Light: Sci. Appl. **4**, e320 (2015).
[5] C. Benko, T. K. Allison, A. Cingöz, L. Hua, F. Labaye, D. C. Yost, and J. Ye, "Extreme ultraviolet radiation with coherence time greater than 1 s," Nat. Photonics **8**, 530–536 (2014).
[6] A. Cingöz, D. C. Yost, T. K. Allison, A. Ruehl, M. E. Fermann, I. Hartl, and J. Ye, "Direct frequency comb spectroscopy in the extreme ultraviolet," Nature **482**, 68–71 (2012).
[7] A. K. Mills, T. J. Hammond, M. H. C. Lam, and D. J. Jones, "XUV frequency combs via femtosecond enhancement cavities," J. Phys. B: At., Mol. Opt. Phys. **45**, 142001 (2012).
[8] C. Gohle, T. Udem, M. Herrmann, J. Rauschenberger, R. Holzwarth, H. A. Schüssler, F. Krausz, and T. W. Hänsch, "A frequency comb in the extreme ultraviolet," Nature **436**, 234–237 (2005).
[9] R. J. Jones, K. D. Moll, M. J. Thorpe, and J. Ye, "Phase-coherent frequency combs in the vacuum ultraviolet via high-harmonic generation inside a femtosecond enhancement cavity," Phys. Rev. Lett. **94**, 193201 (2005).
[10] H. Carstens, M. Högner, T. Saule, S. Holzberger, N. Lilienfein, A. Guggenmos, C. Jocher, T. Eidam, D. Esser, V. Tosa, V. Pervak, J. Limpert, A. Tünnermann, U. Kleineberg, F. Krausz, and I. Pupeza, "High-harmonic generation at 250 MHz with photon energies exceeding 100 eV," Optica **3**(4), 366–369 (2016).
[11] I. Pupeza, S. Holzberger, T. Eidam, H. Carstens, D. Esser, J. Weitenberg, P. Rußbüldt, J. Rauschenberger, J. Limpert, Th. Udem, A. Tünnermann, T. W. Hänsch, A. Apolonski, F. Krausz, and E. Fill, "Compact high-repetition-rate source of coherent 100 eV radiation," Nat. Photonics **7**, 608–612 (2013).
[12] J. Lee, D. R. Carlson, and R. J. Jones, "Optimizing intracavity high harmonic generation for XUV fs frequency combs," Opt. Express **19**(23), 23315–23326 (2011).
[13] D. C. Yost, A. Cingöz, T. K. Allison, A. Ruehl, M. E. Fermann, I. Hartl, and J. Ye, "Power optimization of XUV frequency combs for spectroscopy applications," Opt. Express **19**, 23483 (2011).
[14] P. Rußbüldt, D. Hoffmann, M. Höfer, J. Löhring, J. Luttmann, A. Meissner, J. Weitenberg, M. Traub, T. Sartorius, D. Esser, R. Wester, P. Loosen, and R. Poprawe, "Innoslab amplifiers," IEEE J. Sel. Top. Quantum Electron. **21**, 447 (2015).
[15] O. Pronin, M. Seidel, F. Lücking, J. Brons, E. Fedulova, M. Trubetskov, V. Pervak, A. Apolonski, Th. Udem, and F. Krausz, "High-power multi-megahertz source of waveform-stabilized few-cycle light," Nat. Commun. **6**, 6988 (2015).
[16] C. J. Saraceno, F. Emaury, C. Schriber, A. Diebold, M. Hoffmann, M. Golling, T. Südmeyer, and U. Keller, "Toward millijoule-level high-power ultrafast thin-disk oscillators," IEEE J. Sel. Top. Quantum Electron. **21**, 106 (2015).
[17] A. Ozawa and Y. Kobayash, "VUV frequency-comb spectroscopy of atomic xenon," Phys. Rev. A **87**, 022507 (2013).
[18] T. Saule, S. Heinrich, J. Schötz, N. Lilienfein, M. Högner, O. de Vries, M. Plötner, J. Weitenberg, D. Esser, J. Schulte, P. Rußbüldt, J. Limpert, M. F. Kling, U. Kleineberg, and I. Pupeza, "High-flux, high-photon-energy ultrafast extreme-ultraviolet photoemission spectroscopy at 18.4 MHz pulse repetition rate" (submitted).
[19] C. Corder, P. Zhao, X. Li, M. D. Kershis, A. R. Muraca, M. G. White, and T. K. Allison, "An instrument for time-resolved photoelectron spectroscopy at 87 MHz," in Frontiers in Optics, LM4F.6, 2017.
[20] S. Holzberger, N. Lilienfein, H. Carstens, T. Saule, M. Högner, F. Lücking, M. Trubetskov, V. Pervak, T. Eidam, J. Limpert, A. Tünnermann, E. Fill, F. Krausz, and I. Pupeza, "Femtosecond enhancement cavities in the nonlinear regime," Phys. Rev. Lett. **115**, 023902 (2015).
[21] T. K. Allison, A. Cingöz, D. C. Yost, and J. Ye, "Extreme nonlinear optics in a femtosecond enhancement cavity," Phys. Rev. Lett. **107**, 183903 (2011).
[22] D. R. Carlson, J. Lee, J. Mongelli, E. M. Wright, and R. J. Jones, "Intracavity ionization and pulse formation in femtosecond enhancement cavities," Opt. Lett. **36**(15), 2991–2993 (2011).
[23] O. de Vries, T. Saule, M. Plötner, F. Lücking, T. Eidam, A. Hoffmann, A. Klenke, S. Hädrich, J. Limpert, S. Holzberger, T. Schreiber, R. Eberhardt, I. Pupeza, and A. Tünnermann, "Acousto-optic pulse picking scheme with carrier-frequency-to-pulse-repetition-rate synchronization," Opt. Express **23**(15), 19586–19595 (2015).
[24] J. Limpert, F. Stutzki, F. Jansen, H.-J. Otto, T. Eidam, C. Jauregui, and A. Tünnermann, "Yb-doped large-pitch fibres: Effective single-mode operation based on higher-order mode delocalization," Light: Sci. Appl. **1**, e8 (2012).
[25] T. Saule, S. Holzberger, O. De Vries, M. Plötner, J. Limpert, A. Tünnermann, and I. Pupeza, "Phase- stable, multi-μJ femtosecond pulses from a repetition-rate tunable Ti:Sa-oscillator-seeded Yb-fiber amplifier," Appl. Phys. B **123**, 17 (2017).
[26] G. Scoles, *Atomic and Molecular Beam Methods* (Oxford University Press, 1998), Vol. I, p. 17ff.

[27] O. Schubert, M. Hohenleutner, F. Langer, B. Urbanek, C. Lange, U. Huttner, D. Golde, T. Meier, M. Kira, S. W. Koch, and R. Huber, "Sub-cycle control of terahertz high-harmonic generation by dynamical Bloch oscillations," Nat. Photonics **8**, 119–123 (2014).
[28] T. Luu, M. Garg, S. Kruchinin, A. Moulet, M. Hassan, and E. Goulielmakis, "Extreme ultraviolet high-harmonic spectroscopy of solids," Nature **521**, 498 (2015).
[29] K. F. Lee, X. Ding, T. J. Hammond, M. E. Fermann, G. Vampa, and P. B. Corkum, "Harmonic generation in solids with direct fiber laser pumping," Opt. Lett. **42**, 1113 (2017).